Nigerian Research Journal of Engineering and Environmental Sciences 5(2) 2020 pp. 901-917

Nigerian Research Journal of Engineering and Environmental Sciences
Journal homepage: www.rjees.com

Original Research Article

Application of a New Refined Shear Deformation Theory for the Analysis of Thick Rectangular Plates

***[1]Onyeka, F.C., [1]Osegbowa, D. and [2]Arinze, E.E.**

[1]Department of Civil Engineering, Faculty of Engineering, Edo University Iyamho, Edo State, Nigeria.
[2]Department of Civil Engineering, Faculty of Engineering, Michael Okpara University of Agriculture Umudike, Abia State, Nigeria.
*onyeka.festu@edouniversity.edu.ng

ARTICLE INFORMATION

Article history:
Received 13 Oct, 2020
Revised 28 Oct, 2020
Accepted 29 Oct, 2020
Available online 30 Dec, 2020

Keywords:
Energy method
Trigonometric shear deformation
New refined plate theories
CSSS
Rectangular plate

ABSTRACT

This study presents the application of a new refined plate theory (NRPT) in the static flexural analysis of a rectangular thick plate under uniformly distributed load using the energy method. This new RPT was achieved by incorporating a trigonometric shear deformation theory into a fourth order polynomial–displacement function which was obtained from the principle of elastic theory. The particular plate boundary condition to be analysed is clamped on the third edge and the other three edges simply supported (CSSS). The coefficient of deflection and shear deformation were derived by subjecting the energy equation obtained to direct variation to get the actual deflection, in-plane displacement, normal and shear stresses, moment and stress resultants of the rectangular thick plate. The results obtained from this work was compared with those obtained from other refined plate theories with the same support condition and showed good agreement with those in the literature.

1. INTRODUCTION

Plates are generally well-known structural components in which one dimension (thickness), is much smaller than the other dimensions (length and breaths) (Shwetha *et al.,* 2018). Plates are generally classified based on thickness as: thin plate, moderately thick plate and thick plate (Chandrashekhara, 2001). Also, they are classified based on the nature of deformation and material properties: Orthotropic, isotropic, anisotropic plates etc, and based on shape: rectangular, triangular, circular plates etc. (Nwoji *et al.,* 2017). Thick plates have a wide range of applications due to their advantages such as high mechanical properties, light weight, reduction in cost, heavy loads carrying capacities etc. (Ibearugbulem and Onyeka, 2020). They are used for the construction of civil engineering structures and other industrial applications, likes bridges, roof, floor slabs, retaining walls, turbine disks, railways, ships dams, coaches, aircraft, etc. (Onyeka *et al.,* 2018).

The loads (static flexural and dynamic loads) carried by plates are usually perpendicular to the surface of the plate (Osadebe *et al.,* 2016) and they can have different supports at their edges, which can be fixed, simply supported, point, etc., just as seen in other structural elements like slab, beams, etc. Due to the loads acting on a plate, stresses are developed (Onyeka and Ibearugbulem, 2020).

Classical plate theory (CPT) developed by Kirchhoff (1850) are normally used in plate analysis. In his study, Kirchhoff (1850) assumed that line which is normal to the neutral surface before deformation remain straight and normal on the neutral surface after deformation and it is mainly applied for the analysis of thin plate. This theory did not consider the effect of shear deformation in the analysis. This limitation of CPT in the analysis of thick plates brought about the refined plate theories (RPT), as an improvement to the CPT (Ibearugbulem *et al.,* 2014, 2016).

Some researchers have used some of the RPT in the analysis of plates like: the first order shear deformation (FSDT) which requires shear correction factor to account for good variation of transverse shear stresses along the thickness axes (Lanhe, 2004; Shimpi *et al.,* 2007; Alieldin *et al.,* 2011). Other shear deformation theories formulated, includes second order shear deformation theory (SSDT) (Khdeir and Reddy, 1999; Saidi and Sahraee, 2006), exponential shear deformation theory (ESDT) (Sayyad and Ghugal, 2012), polynomial shear deformation theory (Ozioko *et al.,* 2019; Onyeka and Edozie, 2020), higher order shear deformation theories (HSDT) (Leung *et al.,* 2003; Onyeka *et al.,* 2019) and trigonometric shear deformation theory (TSDT), (Gandhe *et al.,* 2008; Ghugal, and Sayyad, 2010, Shimpi and Ghugal, 2002). trigonometric shear deformation theory (TSDT) was revealed by Soldatos (1992) as theories in which the trigonometric functions relate thickness co-ordinate in the displacement fields of plate and this theory put transverse shear deformation and transverse strain effect into consideration.

It can be observed from the literatures that most studies were based on trigonometric shear deformation theory, exponential shear deformation theory and higher order shear deformation theories. One can rarely find research studies on the analysis of rectangular thick plates based on polynomial shear deformation and trigonometric-displacement functions altogether. Furthermore, the combination of the function is believed to give a more viable and improved model because, the shear deformation is easier to apply unlike the trigonometric whose solution appear tedious. On the order hand, the polynomial displacement function give realistic and close form solution in the bending analysis of plate under such loading configuration. Moreso, more attention has not been given to analysis of thick plate with clamped support at the third edge and the other three edges simply supported. This present work aimed at filling this gap in literature by using the third order polynomial shear deformation theories. Thereafter, the trigonometric-displacement functions is applied to obtain the in-plane displacement, out-of-plane displacement, stresses, moment and stress resultants of rectangular thick plate under uniformly distributed load with clamped support at the third edge and the other three edges simply supported.

2. METHODOLOGY

Following the sketch as presented in Figure 1 and the assumption made as shown below, the governing equation of thick plate under pure bending is made.

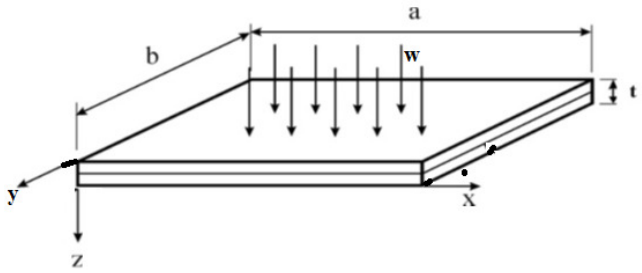

Figure 1: A rectangular thick plate element carrying a uniformly distributed load

2.1. Assumptions

Considering the following assumptions, the general governing equation of a thick rectangular plate will be formulated. They include:

i. The material of the plate is homogeneous, isotropic and elastic.
ii. The stress normal to **x-y** plane is so small that it can be neglected $(\sigma_z = 0)$. That is to say those, the in-plane displacements, u and v are differentiable in x, y and z coordinates, while the deflection (∪) is only differentiable in x and y coordinates i.e., (∪=∪ (x, y).
iii. The effect of the normal strain on the gross response of the plate is small when compared with other strain $(\varepsilon_z = 0)$.
iv. The vertical line that is initially normal to the middle surface of the plate before bending is no longer straight nor normal to the middle surface after bending $(S = S(z))$.

2.2. Kinematics and Constitutive Relationships

In the formulation of the kinematics and constitutive relation, the in-plane displacement components along x-axis (u) and inplane displacement components along y axis (v) are derived (see source (Onyeka *et al.,* 2020) as presented in the Equation (1) and (2):

$$u = \frac{zd\cup}{dx} + S(z).\cap_x \tag{1}$$

$$v = \frac{zd\cup}{dy} + S(z).\cap_y \tag{2}$$

Where, the shear deformation profile of plate section S(z) is given as (Onyeka and Edozie 2020):

$$S(z) = \frac{3}{2}\left(z - \frac{4z^3}{3t^2}\right) \tag{3}$$

$\cap_x$ and $\cap_y$= shear deformation rotation along x and y axis

Considering the assumptions in the previous section (assumption ii), the stress normal to the x-axes gives:

$$\varepsilon_x = \frac{du}{dx} \tag{4}$$

Similarly, the stress normal to the y-axes becomes:

$$\varepsilon_y = \frac{du}{dy} \tag{5}$$

The curvature in x-z plane is defined as:

$$\gamma_{xy} = \frac{du}{dy} + \frac{dv}{dx} \tag{6}$$

The curvature in x-z plane is defined as:

$$\gamma_{xz} = \frac{du}{dz} + \frac{d\cup}{dx} \tag{7}$$

The curvature in x-z plane is defined as:

$$\gamma_{yz} = \frac{dv}{dz} + \frac{d\cup}{dx} \tag{8}$$

The constitutive Equations for five stress and strain components according to Onyeka *et al.* (2020) include:

The normal stress along the direction of x-axes:

$$\sigma_x = \frac{E\left(\varepsilon_x + \mu\varepsilon_y\right)}{1-\mu^2} \tag{9}$$

The normal stress along the direction of y-axes:

$$\sigma_y = \frac{E(\varepsilon_y + \mu\varepsilon_x)}{1-\mu^2} \tag{10}$$

The shear stress along (x-y), (x-z) and (y-z) respectively are given in the Equation (11), (12) and (13) respectively as:

$$\tau_{xy} = \frac{E}{2(1+\mu)} \cdot \gamma_{xy} \tag{11}$$

$$\tau_{xz} = \frac{E}{2(1+\mu)} \cdot \gamma_{xz} \tag{12}$$

$$\tau_{yz} = \frac{E}{2(1+\mu)} \cdot \gamma_{yz} \tag{13}$$

Where:

$\mathrm{E} = \text{Modulus of elasticity and } \mu = \text{poison ratio}$

Substituting Equation (1), (2), (4) and (5) into Equation (9), yields:

$$\sigma_x = \frac{E}{1-\mu^2}\left[\left(-\frac{zd^2\cup}{dx^2} + \frac{Sd\cap_x}{dx}\right) - \mu\left(\frac{zd^2\cup}{dy^2} + \frac{Sd\cap_y}{dy}\right)\right] \tag{14}$$

Substituting Equations (1), (2), (4) and (5) into Equation (10), yields:

$$\sigma_y = \frac{E}{1-\mu^2}\left[\left(-\frac{zd^2\cup}{dy^2} + \frac{Sd\cap_x}{dx}\right) - \mu\left(\frac{zd^2\cup}{dx^2} + \frac{Sd\cap_y}{dy}\right)\right] \tag{15}$$

Substituting Equation (1), (2) and (6) into Equation (11), yields:

$$\tau_{xy} = \frac{E(1-\mu)}{(1-\mu^2)}\left[-\frac{z\partial^2\cup}{\partial x\partial y} + S\left(\frac{d\cap_x}{dy} + \frac{d\cap_y}{dx}\right)\right] \tag{16}$$

Substituting Equation (1), (2) and (7) into Equation (12), yields:

$$\tau_{xz} = \frac{E(1-\mu)}{(1-\mu^2)}\left[\frac{z\partial^2\cup}{\partial x\partial z} + S\left(\frac{d\cap_x}{dz} + \frac{d\cap_z}{dx}\right)\right] \tag{17}$$

Substituting Equation (1), (2) and (8) into Equation (13), yields:

$$\tau_{yz} = \frac{E(1-\mu)}{(1-\mu^2)}\left[\frac{z\partial^2\cup}{\partial y\partial z} + S\left(\frac{d\cap_y}{dz} + \frac{d\cap_z}{dy}\right)\right] \tag{18}$$

2.3. General Energy Equation

The total potential energy expression ($\nexists$), was formulated in accordance to the kinematics and constitutive relation in the previous section (Onyeka *et al.,* 2018).

$$\nexists = \Delta + \nabla \tag{19}$$

Where:

$$\nabla = -\int_0^a \int_0^b w \cup (x,y)\partial x\partial y \tag{20}$$

Where w is the uniformly distributed load.

$$\Delta = \frac{1}{2}\iiint_{-\frac{t}{2}}^{\frac{t}{2}} (\sigma_x\varepsilon_{x+}\sigma_y\varepsilon_{y+}\tau_{xy}\gamma_{xy} + \tau_{xz}\gamma_{xz} + \tau_{yz}\gamma_{yz})dxdydz \tag{21}$$

Thus:

$$\nexists = \frac{D}{2}\int_0^a\int_0^b\left[\left|g_1\left(\frac{\partial^2 \cup}{\partial x^2}\right)^2 - 2g_2\left(\frac{\partial^2 \cup}{\partial x^2}.\frac{\partial \cap_x}{\partial x}\right) + g_3\left(\frac{\partial \cap_x}{\partial x}\right)^2\right|\right.$$
$$+\left|2g_1\left(\frac{\partial^2 \cup}{\partial x\partial y}\right)^2 - 2g_2\left(\frac{\partial^2 \cup}{\partial x\partial y}.\frac{\partial \cap_x}{\partial y}\right) - 2g_2\left(\frac{\partial^2 w}{\partial x\partial y}.\frac{\partial \cap_y}{\partial x}\right)\right|$$
$$+\left|(1+\mu)g_3\left(\frac{\partial \cap_x}{\partial y}\right)\left(\frac{\partial \cap_y}{\partial x}\right)\right| + \frac{(1-\mu)}{2}\left|g_3\left(\frac{\partial \cap_x}{\partial y}\right)^2 + g_3\left(\frac{\partial \cap_y}{\partial x}\right)^2\right|$$
$$+\left|g_1\left(\frac{\partial^2 \cup}{\partial y^2}\right)^2 - 2g_2\left(\frac{\partial^2 \cup}{\partial y^2}.\frac{\partial \cap_y}{\partial y}\right) + g_3\left(\frac{\partial \cap_y}{\partial y}\right)^2\right|$$
$$\left.+\left|\frac{(1-\mu)}{2}g_4(\cap_x)^2 + \frac{(1-\mu)}{2}g_4(\cap_y)^2\right|\right]\partial x\partial y - \int_0^a\int_0^b w \cup (x,y)\partial x\partial y \qquad (22)$$

2.4. Direct Governing Equation

The direct variational method was used to obtain the direct governing differential equation by differentiating the total potential energy with respect to the coefficient of deflection (C), coefficient of shear deformation with respect to x-axis (C_x) and coefficient of shear deformation with respect to y-axis (C_y). The non-dimensional values of quantities along the x and y-axis respectively are presented below.

$$z = ts;\ x = a\ni \text{ and } y = b\in \qquad (23)$$

Where:

a and b = length, breath and thickness of the plate

$\ni, \in$ and s = the non − dimensional value of length, breath and thickness of the plate

Length to breath aspect ratio:

$$\alpha = \frac{b}{a} \qquad (24)$$

Span to thickness ratio:

$$\beta = \frac{a}{t} \qquad (25)$$

Deflection (∪), is the product of shape function of the plate and deflection coefficient:

$$\cup = C.n \qquad (26)$$

Where, n is the shape function of the plate.

The shear deformation rotation along x-axis becomes:

$$\cap_x = \left[\frac{dn}{d\ni}\right][C_x] \qquad (27)$$

The shear deformation rotation along y-axis becomes:

$$\cap_y = \left[\frac{dn}{d\in}\right][C_y] \qquad (28)$$

By substituting Equations 23, 24, 25, 26, 27 and 28 into 22, gives:

$$\nexists = \frac{Et^3}{24(1-\mu^2)a^4}\int_0^1\int_0^1\left[\left|g_1\mathrm{C}^2\left(\frac{\partial^2 n}{\partial \ni^2}\right)^2 - 2g_2\mathrm{C}\mathrm{C}_x\left(\frac{\partial^2 n}{\partial \ni^2}\right)^2 + g_3{\mathrm{C}_x}^2\left(\frac{\partial^2 n}{\partial \ni^2}\right)^2\right|\right.$$
$$+\left|2g_1\frac{\mathrm{C}^2}{\propto^2}\left(\frac{\partial^2 n}{\partial \ni\,\partial \in}\right)^2 - 2g_2\frac{\mathrm{C}\mathrm{C}_x}{\propto^2}\left(\frac{\partial^2 n}{\partial \ni\,\partial \in}\right)^2 - 2g_2\frac{\mathrm{C}\mathrm{C}_y}{\propto^2}\left(\frac{\partial^2 n}{\partial \ni\,\partial \in}\right)^2\right|$$
$$+\left|(1+\mu)g_3\frac{\mathrm{C}_x\mathrm{C}_y}{\propto^2}\left(\frac{\partial^2 h}{\partial \ni\,\partial \in}\right)^2\right| + \frac{(1-\mu)}{2}\left|g_3\frac{{\mathrm{C}_x}^2}{\propto^2}\left(\frac{\partial^2 n}{\partial \ni\,\partial \in}\right)^2 + g_3\frac{{\mathrm{C}_y}^2}{\propto^2}\left(\frac{\partial^2 n}{\partial \ni\,\partial \in}\right)^2\right|$$
$$+\left|g_1\frac{\mathrm{C}^2}{\propto^4}\left(\frac{\partial^2 n}{\partial \in^2}\right)^2 - 2g_2\frac{\mathrm{C}\mathrm{C}_y}{\propto^4}\left(\frac{\partial^2 h}{\partial \in^2}\right)^2 + g_3\frac{{\mathrm{C}_y}^2}{\propto^4}\left(\frac{\partial^2 h}{\partial \in^2}\right)^2\right|$$
$$\left.+\left|\frac{(1-\mu)}{2}\beta^2 g_4{\mathrm{C}_x}^2\left(\frac{\partial n}{\partial \ni}\right)^2 + \frac{(1-\mu)}{2}.\frac{\beta^2 g_4{\mathrm{C}_y}^2}{\propto^2}\left(\frac{\partial n}{\partial \in}\right)^2\right|\right]ab\partial R\partial Q$$
$$-\int_0^1\int_0^1 w\mathrm{C}n\,ab\partial\ni\partial\in \tag{29}$$

Let:

$$s_1 = \int_0^1\int_0^1\left(\frac{d^2 n}{d\ni^2}\right)^2 d\ni d\in \tag{30}$$
$$s_2 = \int_0^1\int_0^1\left(\frac{d^2 n}{d\ni\,d\in}\right)^2 d\ni d\in \tag{31}$$
$$s_3 = \int_0^1\int_0^1\left(\frac{d^2 n}{d\in^2}\right)^2 d\ni d\in \tag{32}$$
$$s_4 = \int_0^1\int_0^1\left(\frac{dn}{d\ni}\right)^2 d\ni d\in \tag{33}$$
$$s_5 = \int_0^1\int_0^1\left(\frac{dn}{d\in}\right)^2 d\ni d\in \tag{34}$$
$$s_6 = \int_0^1\int_0^1 n.d\ni d\in \tag{35}$$

Where the $s_1, s_2, s_3, s_4, s_5\ and\ s_6$ are the stiffness coefficients.
Therefore, differentiating the total potential energy ($\nexists$) with respect to the coefficient of deflection (C), coefficient of shear deformation with respect to x-axis (C_x) and coefficient of shear deformation with respect to y-axis (C_y):

$$\frac{\partial\nexists}{\partial\mathrm{C}} = \frac{\partial\nexists}{\partial\mathrm{C}_x} = \frac{\partial\nexists}{\partial\mathrm{C}_y} = 0 \tag{36}$$

These gives the three Equations of equilibrium as presented in Equation (29), (30) and (31):

$$\int_0^1\int_0^1\left[\mathrm{C}g_1\left(s_1 + \frac{2}{\propto^2}s_2 + \frac{1}{\propto^4}s_3\right) - \mathrm{C}_x g_2\left(s_1 + \frac{1}{\propto^2}s_2\right) - \mathrm{C}_y g_2\left(\frac{1}{\propto^2}s_2 + \frac{1}{\propto^4}s_3\right)\right]d$$
$$\ni d\in = \frac{wa^4}{D}\int_0^1\int_0^1 s_6.d\ni d\in \tag{37}$$

$$\int_0^1\int_0^1\left[-\mathrm{C}g_2\left(s_1+\frac{1}{\propto^2}s_2\right)+\mathrm{C}_x\left(g_3s_1+\frac{(1-\mu)}{2\propto^2}g_3s_2\ +\frac{(1-\mu)}{2}\beta^2g_4s_4\right)+\mathrm{C}_y\frac{(1+\mu)}{2\propto^2}g_3s_2\right]d\ni d\in=0 \tag{38}$$

$$\int_0^1\int_0^1\left[-\mathrm{C}g_2\left(\frac{1}{\propto^2}s_2+\frac{1}{\propto^4}s_3\right)+\mathrm{C}_xg_3\frac{(1+\mu)}{2\propto^2}s_2+\mathrm{C}_yg_3\frac{(1-\mu)}{2}\left(\frac{1}{\propto^2}s_2+\frac{1}{\propto^4}s_3\right)+\mathrm{C}_yg_4\frac{(1-\mu)}{2\propto^2}\beta^2s_5\right]d\ni d\in=0 \tag{39}$$

The three Equations of equilibrium is presented in matrix form as:

$$\begin{bmatrix}t_{11}&t_{12}&t_{13}\\t_{21}&t_{22}&t_{23}\\t_{31}&t_{32}&t_{33}\end{bmatrix}\begin{bmatrix}\mathrm{C}\\\mathrm{C}_x\\\mathrm{C}_y\end{bmatrix}=\frac{wa^4}{D}\begin{bmatrix}s_6\\0\\0\end{bmatrix} \tag{40}$$

Let:

$$t_{11}=g_1\left(s_1+\frac{2}{\propto^2}s_2+\frac{1}{\propto^4}s_3\right) \tag{41}$$

$$t_{12}=-g_2\left(s_1+\frac{1}{\propto^2}s_2\right) \tag{42}$$

$$t_{13}=-g_2\left(\frac{1}{\propto^2}s_2+\frac{1}{\propto^4}s_3\right) \tag{43}$$

$$t_{21}=-g_2\left(s_1+\frac{1}{\propto^2}s_2\right) \tag{44}$$

$$t_{22}=\left(g_3s_1+\frac{(1-\mu)}{2\propto^2}g_3s_2\ +\frac{(1-\mu)}{2}\beta^2g_4s_4\right) \tag{45}$$

$$t_{23}=g_3\frac{(1+\mu)}{2\propto^2}s_2 \tag{46}$$

$$t_{31}=-g_2\left(\frac{1}{\propto^2}s_2+\frac{1}{\propto^4}s_3\right) \tag{47}$$

$$t_{32}=g_3\frac{(1+\mu)}{2\propto^2}s_2 \tag{48}$$

$$t_{33}=\left(g_3\frac{(1-\mu)}{2}\left(\frac{1}{\propto^2}s_2+\frac{1}{\propto^4}s_3\right)+g_4\frac{(1-\mu)}{2\propto^2}\beta^2s_5\right) \tag{49}$$

Solving the matrix in the Equation (40), gives Equations 50, 51 and 52:

$$\mathrm{C}=\frac{wa^4}{D}(k) \tag{50}$$

$$\mathrm{C}_x=\mathrm{C}M_2 \tag{51}$$

$$\mathrm{C}_y=\mathrm{C}M_3 \tag{52}$$

Where:

$$M_2=\frac{t_{21}.t_{33}-t_{23}.t_{31}}{t_{22}.t_{33}-t_{23}.t_{32}} \tag{53}$$

$$M_3=\frac{t_{21}.t_{32}-t_{22}.t_{31}}{t_{23}.t_{32}-t_{22}.t_{33}} \tag{54}$$

$$k=\frac{s_6}{t_{11}M_1-t_{12}M_2-t_{13}M_3} \tag{55}$$

2.5. Displacement, Stresses and Stress Resultant Analysis of the Plate

The expressions for the moment (M_x and M_y), shear force (Q_x and Q_y), in-plane displacement (u and v), deflection ($\cup$) and stress of isotropic rectangular thick plate were derived according to Onyeka and Edozie (2020) by substituting the values of C, C_x and C_y as obtained from the previous section.

Substituting Equation (50) into (26), gave:

$$\cup = \bar{\mathrm{C}}n\left(\frac{wa^4}{D}\right) \tag{56}$$

Where:

$\bar{\mathrm{C}} = k$

$$D = \frac{Et^3}{12(1-\mu^2)} \tag{57}$$

The bending moment along x-axes:

$$M_x = \left(-g_1\bar{\mathrm{C}}\left[\frac{d^2n}{d\ni^2} + \mu\frac{d^2n}{d\in^2}\right] + g_2\left[\overline{\mathrm{C}_x}\frac{d^2n}{d\ni^2} + \mu\overline{\mathrm{C}_y}\frac{d^2n}{d\in^2}\right]\right)wa^2 \tag{58}$$

That is:

$$M_x = \overline{M_x}wa^2 \tag{59}$$

Where:

$$\overline{M_x} = -g_1\bar{\mathrm{C}}\left[\frac{d^2n}{d\ni^2} + \mu\frac{d^2n}{d\in^2}\right] + g_2\left[\overline{\mathrm{C}_x}\frac{d^2n}{d\ni^2} + \mu\overline{\mathrm{C}_y}\frac{d^2n}{d\in^2}\right] \tag{60}$$

Where;

$$\overline{\mathrm{C}_x} = M_2\bar{\mathrm{C}} \tag{61}$$

$$\overline{\mathrm{C}_y} = M_3\bar{\mathrm{C}} \tag{62}$$

The bending moment along y-axes:

$$M_y = \left(-g_1\mathrm{C}\left[\frac{d^2n}{d\in^2} + \mu\frac{d^2n}{d\ni^2}\right] + g_2\left[\overline{\mathrm{C}_y}\frac{d^2n}{d\in^2} + \mu\overline{\mathrm{C}_x}\frac{d^2n}{d\ni^2}\right]\right)wa^2 \tag{63}$$

That is:

$$M_y = \overline{M_y}wa^2 \tag{64}$$

Where;

$$\overline{M_y} = -g_1\mathrm{C}\left[\frac{d^2n}{d\in^2} + \mu\frac{d^2n}{d\ni^2}\right] + g_2\left[\overline{\mathrm{C}_y}\frac{d^2n}{d\in^2} + \mu\overline{\mathrm{C}_x}\frac{d^2n}{d\ni^2}\right] \tag{65}$$

The shear force along x-axes:

$$Q_x = wa\left(-\bar{\mathrm{C}}\left[\frac{\partial^3 n}{\partial\ni^3} + \mu\frac{\partial^3 n}{\partial\in^3}\right] + \left[\overline{\mathrm{C}_x}\frac{\partial^3 n}{\partial\ni^3} + \mu\overline{\mathrm{C}_y}\frac{\partial^3 n}{\partial\in^3}\right]\right) \tag{66}$$

That is:

$$Q_x = \overline{Q_x}wa \tag{67}$$

Where:

$$\overline{Q_x} - \bar{\mathrm{C}}\left[\frac{\partial^3 n}{\partial\ni^3} + \mu\frac{\partial^3 n}{\partial\in^3}\right] + \left[\overline{\mathrm{C}_x}\frac{\partial^3 n}{\partial\ni^3} + \mu\overline{\mathrm{C}_y}\frac{\partial^3 n}{\partial\in^3}\right] \tag{68}$$

The shear force along y-axes:

$$Q_y = wa\left(-\bar{\mathrm{C}}\left[\frac{\partial^3 n}{\partial\ni^3} + \mu\frac{\partial^3 n}{\partial\in^3}\right] + \left[\overline{\mathrm{C}_x}\frac{\partial^3 n}{\partial\ni^3} + \mu\overline{\mathrm{C}_y}\frac{\partial^3 n}{\partial\in^3}\right]\right) \tag{69}$$

That is:

$$Q_y = \overline{Q_y}wa \tag{70}$$

Where:

$$\overline{Q_y} = -\bar{C}\left[\frac{\partial^3 n}{\partial \ni^3} + \mu\frac{\partial^3 n}{\partial \in^3}\right] + \left[\overline{C_x}\frac{\partial^3 n}{\partial \ni^3} + \mu\overline{C_y}\frac{\partial^3 n}{\partial \in^3}\right] \quad (71)$$

The in-plane displacement along x-axes:

$$u = [-\bar{C}s + \overline{C_x}S(s)]\frac{dn}{d\ni}\left(\frac{wa^4}{\beta D}\right) \quad (72)$$

The in-plane displacement along y-axes:

$$v = \frac{1}{\propto}\left[-\bar{C}s + \overline{C_y}S(s)\right]\frac{dn}{d\in}\left(\frac{twa^3}{D}\right) \quad (73)$$

The normal stress along x-axes:

$$\sigma_x = 12\left[[-\bar{C}s + \overline{C_x}S(s)]\frac{d^2 n}{d\ni^2} + \frac{\mu}{\propto^2}\left[-\bar{C}s + \overline{C_y}S(s)\right]\frac{d^2 n}{d\in^2}\right](w\beta^2) \quad (74)$$

The normal stress along y-axes:

$$\sigma_y = w\beta^2\left[12\left[\mu[-\overline{Cs} + C_x S(s)]\frac{d^2 n}{d\ni^2}\right] + \frac{\mu}{\propto^2}\left[-\bar{C}s + \overline{C_y}S(s)\right]\frac{d^2 n}{d\in^2}\right] \quad (75)$$

The shear stress along x-y axes:

$$\tau_{xy} = 6\frac{(1-\mu)}{\propto}\left[-2\bar{C}s + \overline{C_x}S(s) + \overline{C_y}S(s).\frac{1}{\propto}\right]\frac{d^2 n}{\partial\ni\partial\in}(w\beta^2) \quad (76)$$

The shear stress along x-z axes:

$$\tau_{xz} = 6(1-\mu)\overline{C_x}\frac{dS(z)}{dz}\frac{dn}{d\ni}(w\beta^2) \quad (77)$$

The shear stress along y-z axes:

$$\tau_{yz} = \frac{6(1-\mu)}{\propto}\overline{C_y}\frac{dS(z)}{dz}\frac{dn}{d\in}(w\beta^2) \quad (78)$$

2.6. Numerical Problem

The particular shape function for rectangular plate with their respective boundary is shown in Figure 2.

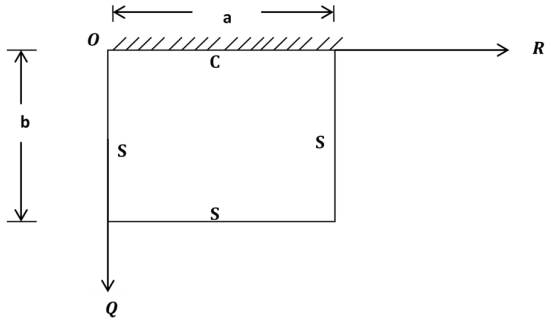

Figure 2: CSSS rectangular plate

Considering Figure 2, the numerical analysis of CSSS rectangular plate at various span-thickness ratios are presented in Table 2. A trigonometric displacement function for the analysis CSSS plate was derived according to Ibearugbulem *et al.* (2019) as presented in Equation 79:

$$\cup_{(\ni,\in)} = \left(a_0 + a_1\ni + a_2 Cos\,(c_1\ni) + a_3 Sin\,(c_1\ni)\right).\left(b_0 + b_1\in + b_2 Cos\,(c_1\in) + b_3 Sin\,(\in)\right) \quad (79)$$

$$\text{At } \ni = \in = 0; \cup = 0 \tag{80}$$

$$\text{At } \ni = \in = 1;\ M_x \text{ and } M_y \left(ie. \frac{d^2\cup}{d\ni^2} = \frac{d^2\cup}{d\in^2} = 0\right) \tag{81}$$

$$\text{At } \ni = \in = 1; \cup = 0 \tag{82}$$

$$\text{At } \in = 0;\ Q_x \text{ and } Q_y \left(ie. \frac{d\cup}{d\in} = 0\right) \tag{83}$$

Substituting Equations (80 to 83) into Equation (79) and solving gives the following constants:

$$Sinf_1 = 0;\ 2Cos\ f_1 + f_1 Sin\ f_1 - 2 \tag{84}$$

The value of f_1 that satisfies Equation (84) is:

$$f_{1_1} = m\pi\ [where\ m = 1, 2, 3 \ldots];\ f_1 = 4.49340946 \tag{85}$$

Substituting Equation (85) into 79 aand its differentials thereby satisfying the boundary conditions of equation (80 to 84) gave;

$$a_0 = a_1 = a_2 = 0;\ b_0 = f_1 b_3;\ b_0 = -f_1 b_3 \tag{86}$$

Substituting the constants of Equation (86) into Equation (79) gives:

$$\cup = a_3 Sin(\pi \ni .) \times b_3 (f_1 - f_1 \in -f_1 Cos\ f_1 \in + Sin\ f_1 \in) \tag{87}$$

That is:

$$\cup = a_3 \times b_3\ (Sin\ \pi \ni).(f_1 - f_1 \in -f_1 Cos\ f_1 \in + Sin\ f_1 \in) \tag{88}$$

Recall from Equation 26, that:

$\cup = n.C$

Therefore:

Let the amplitude:

$$\mathbb{C} = a_3 \times b_3 \tag{89}$$

And:

$$n = (Sin\ \pi \ni).(f_1 - f_1 \in -f_1 Cos\ f_1 \in + Sin\ f_1 \in) \tag{90}$$

Therefore:

$$\cup = (Sin\ \pi \ni).(f_1 - f_1 \in -f_1 Cos\ f_1 \in + Sin\ f_1 \in).\mathbb{C} \tag{91}$$

3. RESULTS AND DISCUSSIONS

The numerical results of stiffness coefficient of the plate are obtained from Equation (30) to (35). It was observed that the values of the stiffness coefficient using the present theory, the new refined plate theory (NRPT) produces a very higher value when compared to Gwarah (2019). Table 2 contains the result of bending moment, shear force and their resultants of a square CSSS rectangular plate at different span to thickness aspect ratio. These numerical values were obtained from the Equation (56) to (71). Studying the results as presented in the Tables 2, it is seen that the non-dimensional out-of-plane displacement ($\cup$), bending moment (M_x and M_y) and shear force (Q_x and Q_y) decreased as the span to thickness ratio increases. This decrement continue until failure occurs in the plate structure. This means that, the load that causes the plate to deflect also causes the plate material to bend simultaneously.

From a critical look at Table 3, and studying the results as presented in the Tables 2 to 5, it is shown that the non-dimensional displacement (u, v and $\cup$) characteristics decrease with increases in the value of the span-thickness ratio. It is also observed in the Tables that the displacement (u, v and $\cup$) and stresses characteristics

increase as the value of the length to breadth ratio increases. This means that, the in-plane displacement are functions of x, y and z as it varies with the plate thickness while the deflection is only a function of x and y and did not varies linearly with the thickness of the plate thickness. Similarly, it was deduced that the normal stress ($\sigma_x \; and \; \sigma_y$) and shear stress characteristics ($\tau_{xy}, \tau_{xz} \; and \; \tau_{yz}$) also decrease as the span-thickness ratio increases. It is also observed in the Table 3 that the stresses characteristics ($\sigma_x, \sigma_y, \tau_{xy}, \tau_{xz} \; and \; \tau_{yz}$)increase as the value of the length to breadth ratio increases. It is observed that, at span to thickness ratio between 4 and 20, the value of vertical shear stress along y and z axes (τ_{yz}) varies between 0.00312 and 0.000122. These values of vertical shear stress become 7.8E-05 and 1.15E-05 at the span to thickness between 25 and 65 respectively. Meanwhile, the value of vertical shear stress (τ_{yz}) is about 9.94E-06 and 4.87E-06, at the span to thickness between 70 and 100 which is about 0.0000001 when corrected to 5 decimal places. The value becomes almost constant or equal to the value from CPT.

Table 1: Values of stiffness coefficient, s for various support (boundary conditions)

Theory	Plate	s_1	s_2	s_3	s_4	s_5	s_6
Gwarah (2019)	CSSS	0.036191	0.041633	0.000371	0.003662	0.004218	0.015000
Present (NRPT)	CSSS	928.2428	1,015.280	2,057.980	94.05066	102.8692	2.381387

Table 2: Bending moments, shear force and stress resultants of CSSS plate for b/a = 1. 0

β	∪ (m) $\overline{\cup}$	$M_x\,(kNm)$ $\overline{M_x}$	$M_y(kNm)$ $\overline{M_y}$	$Q_x\,(kN)$ $\overline{Q_x}$	$Q_y\,(kN)$ $\overline{Q_y}$
4	0.006435	0.635110	0.795993	0.371070	0.751446
5	0.005870	0.638890	0.771027	0.321232	0.658649
6	0.005568	0.640918	0.757632	0.294517	0.608913
7	0.005386	0.642133	0.749611	0.278528	0.579148
8	0.005269	0.642917	0.744427	0.268198	0.559920
9	0.005189	0.643454	0.740883	0.261138	0.546777
10	0.005132	0.643837	0.738353	0.256098	0.537397
15	0.004997	0.644742	0.732377	0.244198	0.501830
20	0.004950	0.645058	0.730291	0.240045	0.499975
25	0.004928	0.645204	0.729326	0.238125	0.499117
30	0.004916	0.645283	0.728802	0.237082	0.498651
35	0.004909	0.645331	0.728487	0.236453	0.498370
40	0.004904	0.645362	0.728282	0.236046	0.498188
45	0.004901	0.645383	0.728141	0.235766	0.498063
50	0.004899	0.645398	0.728041	0.235566	0.497974
55	0.004897	0.645409	0.727967	0.235418	0.497908
60	0.004896	0.645418	0.727910	0.235306	0.497858
65	0.004896	0.645425	0.727866	0.235218	0.497819
70	0.004894	0.645430	0.727831	0.235149	0.497788
80	0.004893	0.645438	0.727780	0.235047	0.497742
85	0.004893	0.645441	0.727761	0.235009	0.497725
90	0.004893	0.645443	0.727745	0.234977	0.497711
95	0.004893	0.645445	0.727731	0.234950	0.497699
100	0.004892	0.645447	0.727720	0.234927	0.497688
CPT	0.004890	0.645463	0.727614	0.046943	0.497594

In summary, there are three categories of rectangular plates. The plates whose vertical shear stress do not vary well from zero will be classified as thin plates because its value is almost equal to the value of the CPT.

In between the thin and thick plate is the classified as moderate thick plate. Since the plate whose transverse shear stress varies very much from zero is categorized as thick plates. Therefore, the span-to-depth ratio for these categories of rectangular plates are: Thick plate:$a/t \leq 20$; moderately thick plate: $25 \leq a/t \leq 65$; thin plate: $a/t \geq 70$. This confirmation can be used to show the boundary between thin and thick plate. Thus, it can be deduced from this research work that thick plate is the one whose span-depth ratio value is 4 up to 20.

Studying the results as presented in the Tables 2 to 5, it is shown that the non-dimensional displacement (u, v and ∪) characteristics decrease with increases in the value of the span-thickness ratio. It is also observed in the Tables that the displacement (u, v and ∪) and stresses characteristics increase as the value of the length to breadth ratio increases. This means that, the in-plane displacement are functions of x, y and z as it varies with the plate thickness while the deflection is only a function of x and y and did not varies linearly with the thickness of the plate thickness.

Similarly, it was deduced that the normal stress ($\sigma_x \; and \; \sigma_y$) and shear stress characteristics ($\tau_{xy}, \tau_{xz} \; and \; \tau_{yz}$) also decrease as the span-thickness ratio increases. It is also observed in the Table 3 that the stresses characteristics $\left(\sigma_x, \sigma_y, \tau_{xy}, \tau_{xz} \; and \; \tau_{yz}\right)$increase as the value of the length to breadth ratio increases.

Table 3: Displacement and stresses of CSSS plate for length to breadth ratio of 1.0

β	∪ (m) $\bar{\cup}$	$u\,(m)$ $\bar{u}$	$v\,(m)$ $\bar{v}$	σ_x $\overline{\sigma_x}$	σ_y $\overline{\sigma_y}$	$\tau_{xy}\,(kN$ $\overline{\tau_{xy}}$	$\tau_{xz}(kN/m)$ $\overline{\tau_{xz}}$	τ_{yz} $\overline{\tau_{yz}}$
4	0.006436	-0.008609	-0.002970	0.438250	0.520710	-0.076080	0.021274	0.003120
5	0.005871	-0.008322	-0.002778	0.419620	0.489967	-0.072294	0.013500	0.001979
6	0.005568	-0.008168	-0.002675	0.409633	0.473483	-0.070264	0.009332	0.001368
7	0.005387	-0.008076	-0.002614	0.403657	0.463615	-0.069050	0.006838	0.001002
8	0.005270	-0.008017	-0.002574	0.399795	0.457239	-0.068265	0.005226	0.000766
9	0.005190	-0.007976	-0.002547	0.397156	0.452881	-0.067728	0.004124	0.000604
10	0.005132	-0.007947	-0.002527	0.395272	0.449770	-0.067345	0.003338	0.000489
15	0.004997	-0.007878	-0.002482	0.390823	0.442423	-0.066441	0.001480	0.000217
20	0.004950	-0.007854	-0.002465	0.389271	0.439859	-0.066125	0.000832	0.000122
25	0.004929	-0.007843	-0.002458	0.388553	0.438674	-0.065979	0.000532	7.80E-05
30	0.004916	-0.007837	-0.002454	0.388163	0.438030	-0.065900	0.000370	5.41E-05
35	0.004910	-0.007834	-0.002452	0.387928	0.437642	-0.065852	0.000272	3.98E-05
40	0.004905	-0.007831	-0.002450	0.387776	0.437390	-0.065821	0.000208	3.04E-05
45	0.004902	-0.007830	-0.002449	0.387671	0.437217	-0.065800	0.000164	2.41E-05
50	0.004900	-0.007829	-0.002448	0.387596	0.437094	-0.065785	0.000133	1.95E-05
55	0.004898	-0.007828	-0.002448	0.387541	0.437003	-0.065773	0.000110	1.61E-05
60	0.004896	-0.007827	-0.002447	0.387499	0.436933	-0.065765	9.24E-05	1.35E-05
65	0.004896	-0.007827	-0.002447	0.387466	0.436879	-0.065758	7.87E-05	1.15E-05
70	0.004895	-0.007826	-0.002447	0.387440	0.436836	-0.065753	6.79E-05	9.94E-06
75	0.004894	-0.007826	-0.002446	0.387402	0.436773	-0.065745	5.20E-05	7.61E-06
80	0.004894	-0.007826	-0.002446	0.387402	0.436773	-0.065745	5.20E-05	7.61E-06
90	0.004893	-0.007825	-0.002446	0.387376	0.436730	-0.065740	4.11E-05	6.01E-06
95	0.004893	-0.007825	-0.002446	0.387366	0.436713	-0.065738	3.68E-05	5.40E-06
100	0.004892	-0.007825	-0.002446	0.387357	0.436699	-0.065736	3.33E-05	4.87E-06
CPT	0.004890	-0.007824	-0.002445	0.387279	0.436569	-0.065720	3.33E-07	4.87E-08

Looking closely at Table 4, it can be seen that at span to thickness ratio between 4 and 15, the value of vertical shear stress along y and z axes τ_{yz} varies 0.024274 and 0.001701. These values of vertical shear stress become 0.000956 and 0.000106 in the span to a thickness between 20 and 60 respectively. Meanwhile, the value of vertical shear stress τ_{yz} is about 9.05E-05 and 3.82E-05, in the span to a thickness between 65 and 100, which is about 0.000001 when corrected to 5 decimal places. The value become almost constant or equal to the value from CPT.

Table 4: Displacement and stresses of CSSS plate for length to breadth ratio of 1.5

β	∪ (m)	$u\ (m)$	$v\ (m)$	σ_x (kN/m)	$\sigma_y(kN/m)$	τ_{xy} (kN/m)	$\tau_{xz}(kN/m)$	τ_{yz} (kN/m)
	$\bar{U}$	$\bar{u}$	$\bar{v}$	$\overline{\sigma_x}$	$\overline{\sigma_y}$	$\overline{\tau_{xy}}$	$\overline{\tau_{xz}}$	$\overline{\tau_{yz}}$
4	0.008983	0.009983	-0.014050	-0.003059	0.593768	0.445327	-0.080438	0.024274
5	0.008260	0.009260	-0.013590	-0.002916	0.573222	0.426708	-0.077243	0.015445
6	0.008171	0.008871	-0.013340	-0.002839	0.562180	0.416677	-0.075523	0.010692
7	0.008087	0.008638	-0.013200	-0.002793	0.555562	0.410655	-0.074491	0.007840
9	0.007584	0.008384	-0.013040	-0.002742	0.548357	0.404091	-0.073366	0.004733
10	0.007309	0.008310	-0.012990	-0.002728	0.546267	0.402186	-0.073040	0.003832
15	0.007135	0.008134	-0.012880	-0.002693	0.541330	0.397682	-0.072268	0.001701
20	0.007075	0.008075	-0.012840	-0.002681	0.539605	0.396109	-0.071998	0.000956
25	0.008047	0.008047	-0.012830	-0.002676	0.538808	0.395381	-0.071874	0.000612
30	0.007031	0.008032	-0.012820	-0.002673	0.538375	0.394985	-0.071806	0.000425
35	0.007022	0.008022	-0.012810	-0.002671	0.538114	0.394747	-0.071765	0.000312
40	0.007016	0.008016	-0.012810	-0.002670	0.537945	0.394592	-0.071739	0.000239
45	0.007012	0.008012	-0.012800	-0.002669	0.537829	0.394486	-0.071721	0.000189
50	0.007009	0.008009	-0.012800	-0.002668	0.537746	0.394411	-0.071708	0.000153
55	0.007007	0.008007	-0.012800	-0.002668	0.537684	0.394354	-0.071698	0.000126
60	0.007006	0.008006	-0.012800	-0.002667	0.537638	0.394312	-0.071691	0.000106
65	0.007004	0.008004	-0.012800	-0.002667	0.537601	0.394279	-0.071685	9.05E-05
70	0.007003	0.008003	-0.012800	-0.002667	0.537572	0.394252	-0.071680	7.80E-05
75	0.007002	0.008002	-0.012800	-0.002667	0.537530	0.394214	-0.071674	5.97E-05
80	0.007002	0.008002	-0.012800	-0.002667	0.537530	0.394214	-0.071674	5.97E-05
90	0.007001	0.008001	-0.012800	-0.002666	0.537501	0.394187	-0.071669	4.72E-05
95	0.008000	0.008000	-0.012800	-0.002666	0.537490	0.394177	-0.071668	4.23E-05
100	0.007000	0.008000	-0.012800	-0.002666	0.537480	0.394168	-0.071666	3.82E-05
CPT	0.006997	0.007997	-0.012800	-0.002666	0.537393	0.394088	-0.071652	3.82E-07

In summary, there are three categories of rectangular plates. The plates whose vertical shear stress do not vary well from zero will be classified as thin plates because its value is almost equal to the value of the CPT. In between the thin and thick plate is the classified as moderate thick plate. Since the plate whose transverse shear stress varies very much from zero is categorized as thick plates. Therefore, the span-to-depth ratio for these categories of rectangular plates are: Thick plate:$a/t \leq 15$; moderately thick plate: $20 \leq a/t \leq 60$; thin plate: $a/t \geq 65$. This confirmation can be used to show the boundary between thin and thick plate. Thus, it can be deduced from this research work that thick plate is the one whose span-depth ratio value is 4 up to 15.

Studying the results as presented in the Tables 5, it is shown that the non-dimensional displacement (u, v and ∪) characteristics decrease with increases in the value of the span-thickness ratio. It is also observed in the Tables that the displacement (u, v and ∪) and stresses characteristics increase as the value of the length to breadth ratio increases. This means that, the in-plane displacement are functions of x, y and z as it varies

with the plate thickness while the deflection is only a function of x and y and did not varies linearly with the thickness of the plate thickness.

Table 5: Displacement and stresses of CSSS plate for length to breadth ratio of 2.0

β	$\cup(m)$	$u\ (m)$	$v\ (m)$	$\sigma_x\ (kN/m)$	$\sigma_y(kN/m)$	τ_{xy} (kN/m)	$\tau_{xz}(kN/m)$	τ_{yz} (kN/m)
	$\bar{U}$	$\bar{u}$	$\bar{v}$	$\overline{\sigma_x}$	$\overline{\sigma_y}$	$\overline{\tau_{xy}}$	$\overline{\tau_{xz}}$	$\overline{\tau_{yz}}$
4	0.012551	-0.017975	-0.002879	0.709286	0.401445	-0.076446	0.026544	-0.017975
5	0.011723	-0.017415	-0.002767	0.686712	0.387293	-0.073758	0.016896	-0.017415
6	0.011277	-0.017114	-0.002706	0.674569	0.379664	-0.072308	0.011698	-0.017114
7	0.011009	-0.016934	-0.002669	0.667286	0.375083	-0.071438	0.008580	-0.016934
8	0.010836	-0.016817	-0.002646	0.662576	0.372118	-0.070875	0.006561	-0.016817
9	0.010718	-0.016738	-0.002629	0.659353	0.370088	-0.070489	0.005180	-0.016738
10	0.010633	-0.016681	-0.002618	0.657052	0.368639	-0.070214	0.004194	-0.016681
15	0.010434	-0.016546	-0.002590	0.651613	0.365210	-0.069562	0.001861	-0.016546
20	0.010364	-0.016499	-0.002581	0.649714	0.364012	-0.069335	0.001047	-0.016499
25	0.010332	-0.016477	-0.002576	0.648835	0.363458	-0.069230	0.000670	-0.016477
30	0.010314	-0.016466	-0.002574	0.648358	0.363157	-0.069172	0.000465	-0.016466
40	0.010297	-0.016454	-0.002572	0.647884	0.362858	-0.069116	0.000261	-0.016454
45	0.010292	-0.016451	-0.002571	0.647756	0.362778	-0.069100	0.000207	-0.016451
50	0.010289	-0.016448	-0.002571	0.647665	0.362720	-0.069089	0.000167	-0.016448
55	0.010286	-0.016447	-0.002570	0.647597	0.362677	-0.069081	0.000138	-0.016447
60	0.010284	-0.016445	-0.002570	0.647545	0.362645	-0.069075	0.000116	-0.016445
65	0.010283	-0.016444	-0.002570	0.647505	0.362619	-0.069070	9.90E-05	-0.016444
70	0.010282	-0.016444	-0.002570	0.647474	0.362599	-0.069066	8.54E-05	-0.016444
75	0.010280	-0.016442	-0.002569	0.647427	0.362570	-0.069061	6.54E-05	-0.016442
80	0.010280	-0.016442	-0.002569	0.647427	0.362570	-0.069061	6.54E-05	-0.016442
85	0.010279	-0.016442	-0.002569	0.647410	0.362559	-0.069059	5.79E-05	-0.016442
90	0.010279	-0.016442	-0.002569	0.647395	0.362550	-0.069057	5.17E-05	-0.016442
95	0.010278	-0.016441	-0.002569	0.647383	0.362542	-0.069056	4.64E-05	-0.016441
100	0.010278	-0.016441	-0.002569	0.647372	0.362535	-0.069054	4.18E-05	-0.016441
CPT	0.010274	-0.016439	-0.002569	0.647276	0.362474	-0.069043	4.18E-07	-0.016439

Similarly, it was deduced that the normal stress $(\sigma_x\ and\ \sigma_y)$ and shear stress characteristics $(\tau_{xy}, \tau_{xz}\ and\ \tau_{yz})$ also decrease as the span-thickness ratio increases. It is also observed in the Table 3 that the stresses characteristics $(\sigma_x, \sigma_y, \tau_{xy}, \tau_{xz}\ and\ \tau_{yz})$increase as the value of the length to breadth ratio increases. These decrements continue until failure occurs in the plate structure.

Furthermore, from Table 5 it can be seen that at span to a thickness ratio between 4 and 20, the value of vertical shear stress along y and z axes (τ_{xz}) varies between 0.0265441 and 0.0010465. These values of vertical shear stress become 0.0006696 and 0.0001162 in the span to a thickness between 25 and 60 respectively. Meanwhile, the value of vertical shear stress (τ_{yz}) is about 9.902E-05 and 4.184E-05, in the span to a thickness between 65 and 100 which is about 0.000001 when corrected to 5 decimal places. The value become almost constant or equal to the value from CPT.

In summary, there are three categories of rectangular plates. The plates whose vertical shear stress do not vary well from zero will be classified as thin plates because its value is almost equal to the value of the CPT. In between the thin and thick plate is the classified as moderate thick plate. Since the plate whose transverse

shear stress varies very much from zero is categorized as thick plates. Therefore, the span-to-depth ratio for these categories of rectangular plates are: Thick plate:$a/t \leq 20$; moderately thick plate: $25 \leq a/t \leq 60$; thin plate: $a/t \geq 65$. This confirmation can be used to show the boundary between thin and thick plate. Thus, it can be deduced from this research work that thick plate is the one whose span-depth ratio value is 4 up to 20.

The result of the comparison made as presented in Table 6, shows that the present study predicts slightly higher values for all aspect ratios. This proves some level safety and reliability of this method as it will not put the structure into danger. The total average percentage difference between the present study and that of Gwarah (2019) is 8.1%. This means that at the 92 % confidence level, the values from the present study are the same with those from of previous studies. This value has been sufficient in the statistical analysis showed that the present method can be used with confidence for analysis of deflection on a CSSS rectangular plate.

Table 6: Comparison of results from the present work and literature values for length to width ratio of 1.5

β	Present work ∪ (m)	Gwarah, (2019) ∪ (m)	Percentage difference (%)
4	0.008983	0.008369	7.340356
5	0.008260	0.007684	7.490897
10	0.007310	0.006767	8.017295
20	0.007075	0.006537	8.2233
30	0.007032	0.006495	8.265253
40	0.007016	0.006480	8.280271
50	0.007009	0.006472	8.287244
60	0.007006	0.006469	8.290966
70	0.007003	0.006467	8.293412
80	0.007001	0.006465	8.294821
90	0.007001	0.006464	8.295962
100	0.007000	0.006464	8.296577
CPT	0.006997	-	-
Average % difference		8.114696	
Total % difference		8.1	

4. CONCLUSION

Application of a new refined shear deformation theory for the analysis of thick rectangular plate has been investigated. From the study this conclusion has been drawn:

i. The in-plane displacement, deflection, moment, shear force and stresses decrease with increases in the value of the span-thickness ratio.
ii. The displacement (u and v and ∪) and stresses characteristics ($\sigma_x, \sigma_y, \tau_{xy}, \tau_{xz}\ and\ \tau_{yz}$) increase as the value of the length to breadth ratio increases.
iii. The constitutive relations are satisfied in respect of in-plane stress and transverse shear stress while predicting the flexural characteristics of the plate. The theory which includes the effects of transverse shear deformations did not require shear correction factor which is associated to first order shear deformation theory.
iv. The governing differential equations and associated boundary conditions obtained are variationally consistent and can be used with confidence in the analysis of isotropic rectangular.
v. The deflection and stresses obtained by present theory are in good agreement with the other order theories. This validates the efficacy and reliability of the present new refined plate theory (NRPT).

5. CONFLICT OF INTEREST

There is no conflict of interest associated with this work.

REFERENCES

Alieldin, S.S., Alshorbagy, A.E. and Shaat A. M. (2011). First-order shear deformation finite element model for elastostatic analysis of laminated composite plates and the equivalent functionally graded plates. *Ain Shams Engineering Journal*, 2, pp. 53 – 62.

Chandrashekhara K. (2001). *Theory of Plates*. University Press (India) Limited.

Gandhe, G.R., Salve, S.B., Pankade P.M. and Taur, P.G. and Tupe, D.H. (2018). Trigonometric Shear Deformation Theory for Thermal Flexural Analysis of Isotropic Plate. *2nd International Conference on Materials Manufacturing and Design Engineering, Procedia Manufacturing,* 20, pp. 499–504.

Ghugal, Y. M. and Sayyad, A. S. (2010). A static flexure of thick isotropic plates using trigonometric shear deformation theory. *Journal of Solid Mechanics*, 2(1), pp. 79–90.

Gwarah, L. S. (2019). Application of shear deformation theory in the analysis of thick rectangular plates using polynomial displacement functions. *PhD Thesis, Department of Civil Engineering, Federal University of Technology, Owerri, Nigeria.*

Ibearugbulem, O.M., Ezeh, J. C. and Ettu, L. O. (2014). *Energy methods in theory of rectangular plates (use of polynomial shape functions).* Liu House of Excellence Ventures, Owerri, pp. 10 – 20.

Ibearugbulem, O. M., Njoku, K.O. and Eziefula, U.G. (2016). Full Shear Deformation for Analysis of Thick Plate. *Proceedings of Academics World 43rd International Conference, Rome, Italy*.

Ibearugbulem, O. M., Onyechere, I. C., Ezeh, J. C. and Anya, U. C. (2019). Determination of Exact Displacement Functions for Rectangular Thick Plate Analysis. *FUTO Journal Series (FUTOJNLS)*, 5(1), pp. 101 – 116.

Ibearugbulem, O. M. and Onyeka, F. C. (2020). Moment and Stress Analysis Solutions of Clamped Rectangular Thick Plate. *European Journal of Engineering Research and Science,* 5(4), pp. 531 - 534.

Khdeir, A.A. and Reddy, J.N. (1999). Free vibrations of laminated composite plates using second order shear deformation theory. *Computers and Structures,* 71, pp. 617 - 626.

Kirchhoff, G. R. (1850). U''ber das Gleichgewicht and die Bewegung einer elastschen Scheibe. *Journal f'' ur die reine und angewandte Mathematik,* 40, pp. 51 - 88 (in German).

Lanhe, W. (2004). Thermal buckling of a simply supported moderately thick rectangular FGM plate. *Composite Structures,* 64, pp. 211 – 8.

Leung, A. Y. T., Niu, J., Lim, C. W. and Song, K. (2003). A new unconstrained third-order plate theory for Navier solutions of symmetrically laminated plates. *Computers and Structures,* 81, pp. 2539 – 2548.

Nwoji C.U., Mama B.O., Onah H.N., Ike C.C. (2017). Kantorovich-Vlasov Method for Simply Supported Rectangular Plates under Uniformly Distributed Transverse Loads. *International Journal of Civil, Mechanical and Energy Science (IJCMES),* 3(2), pp. 69 - 77.

Onyeka, F.C. and Edozie, O. T. (2020). Application of Higher Order Shear Deformation Theory in the Analysis of thick Rectangular Plate. *International Journal on Emerging Technologies,* 11(5), pp. 62–67.

Onyeka, F. C., Okafor, F.O. and Onah, H. N. (2018). Displacement and Stress Analysis in Shear Deformable Thick Plate. *International Journal of Applied Engineering Research,* 13(11), pp. 9893 – 9908.

Onyeka, F. C., Okafor, F.O. and Onah, H.N. (2019). Application of Exact Solution Approach in the Analysis of Thick Rectangular Plate. *International Journal of Applied Engineering Research*, 14(8), pp. 2043 – 2057.

Onyeka, F.C., Okeke T. E and Wasiu, J. (2020). Strain–Displacement Expressions and their Effect on the Deflection and Strength of Plate. *Advances in Science, Technology and Engineering Systems,* 5(5), pp. 401-413 (2020).

Osadebe N.N., Ike C.C., Onah H. N, Nwoji C.U., and Okafor F.O. (2016). Application of the Galerkin-Vlasov Method to the Flexural Analysis of Simply Supported Rectangular Kirchhoff Plates under Uniform Loads. *Nigerian Journal of Technology, NIJOTECH*, 35(4), pp. 732 – 738.

Ozioko, H.O., Ibearugbulem, O.M., Ezeh, J.C. and Anya, U.C. (2019). Algorithm for Exact Solution of Thick Anisotropic Plates. *Scholars Journal of Applied Scientific Research*, 2(4), pp. 11 - 25.

Saidi, A.R. and Sahraee, S. (2006). Axisymmetric solutions of functionally graded circular and annular plates using second-order shear deformation plate theory. *ESDA2006-95699, 8th Biennial ASME Conference on Engineering Systems Design and Analysis, Torino, Italy.*

Sayyad, A.S. and Ghugal, Y.M. (2012). Bending and Free Vibration Analysis of thick isotropic plates by using exponential shear deformation theory. *Applied and Computational Mechanics,* 6(1), pp. 65–82.

Shimpi, R. P. and Ghugal, Y. M. (2002). A layer wise shear deformation theory for two layered cross-ply laminated plates. *Mechanics of Composite Materials and Structures: An International Journal* 7(4), pp. 331–353.

Shimpi, R. P., Patel, H. G. and Arya, H. (2007). New first order shear deformation plate theories. *Journal of Applied Mechanics* 74, pp. 523 – 533.

Shwetha, K., Subrahmanya, V. and Bhat, P., (2018). Comparison Between Thin Plate and Thick Plate From Navier Solution Using Matlab Software. *International Research Journal of Engineering and Technology (IRJET),* 5(6), pp. 2675 – 2680.

Soldatos, K. P. (1992). A transverse shear deformation theory for homogeneous monoclinic plates. *Acta Mechanica,* 94, pp. 195 – 220.